

Inductive Attention for Video Action Anticipation

Tsung-Ming Tai^{1,2}, Giuseppe Fiameni¹, Cheng-Kuang Lee¹, Simon See¹, Oswald Lanz²

¹NVIDIA AI Technology Center ²Free University of Bozen-Bolzano

{ntai, gfiameni, ckl, ssee}@nvidia.com {tstai, oswald.lanz}@unibz.it

Abstract

Anticipating future actions based on spatiotemporal observations is essential in video understanding and predictive computer vision. Moreover, a model capable of anticipating the future has important applications, it can benefit precautionary systems to react before an event occurs. However, unlike in the action recognition task, future information is inaccessible at observation time – a model cannot directly map the video frames to the target action to solve the anticipation task. Instead, the temporal inference is required to associate the relevant evidence with possible future actions. Consequently, existing solutions based on the action recognition models are only suboptimal. Recently, researchers proposed extending the observation window to capture longer pre-action profiles from past moments and leveraging attention to retrieve the subtle evidence to improve the anticipation predictions. However, existing attention designs typically use frame inputs as the query which is suboptimal, as a video frame only weakly connects to the future action. To this end, we propose an inductive attention model, dubbed IAM, which leverages the current prediction priors as the query to infer future action and can efficiently process the long video content. Furthermore, our method considers the uncertainty of the future via the many-to-many association in the attention design. As a result, IAM consistently outperforms the state-of-the-art anticipation models on multiple large-scale egocentric video datasets while using significantly fewer model parameters.

1. Introduction

Recognizing human actions from videos has been extensively studied in video understanding [5, 21, 59, 11, 34, 23, 52, 35, 53, 54]. Since the input observations are aligned in time with their action annotations, the action recognition models can learn the direct mapping of the video context to the action semantics. Besides, unlike action recognition, early action recognition fore-

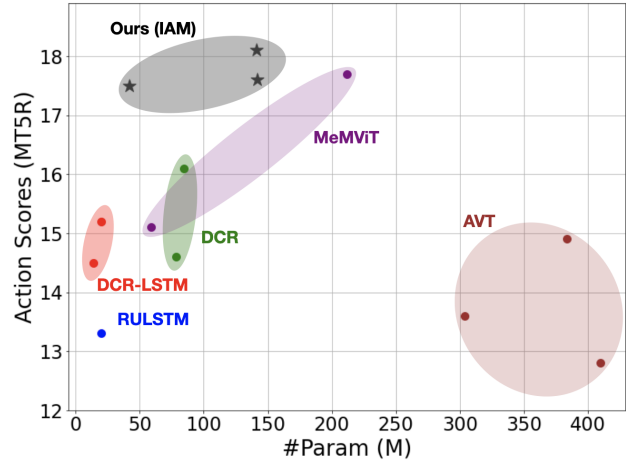


Figure 1. **Inductive Attention Model (IAM)** achieves higher action anticipation accuracy with fewer parameters. Here we compare IAM to previous methods on the EPIC-Kitchens-100 dataset. (Multiple points indicate model variants using different backbones.)

sees the action with incomplete observations of input videos; the models only rely on initial frames to describe an action [51, 60, 20, 32, 1, 40]. Although early action recognition models are capable of detecting an activity as early as possible, the partial observations of action is still required as inputs. Therefore for some applications, such as precautionary systems [2, 46, 45] that must plan before an event occurs, early action recognition could not satisfy the requirements.

Video action anticipation, on the other hand, aims to predict near-future actions based on disjoint pre-action intervals [24, 41]. In this case, action is completely hidden from the supporting video input, leading to different challenges than in the action recognition or early action recognition tasks. For example, observations can no longer describe an action but only hint to the occurrence of specific further action. Furthermore, similar pre-actions could lead to different possible consequence actions, where the uncertainty of the

future reveals a many-to-many association rather than a one-to-one mapping. As a result, action anticipation is more akin to causal inference than to pattern recognition. Addressing the anticipation task with existing recognition models is suboptimal.

The advent of transformers contributed to the achievement of remarkable performance in action anticipation [22, 61]. Recent work [61] proposes using a more extended context to compensate for insufficient information on pre-action intervals and shows improving accuracy in action anticipation. However, the underlying design remained unchanged from that of action recognition. One of the critical design choices in attention models is the selection of an appropriate query that triggers the discovery of valuable features. A widely adopted option is to take the incoming frame as the input query in sequential order. However, querying by observing may be less effective and an indirect usage, considering the weak connection between the video content and anticipation labels.

An alternative, and in this context arguably more grounded choice for the query is to leverage the last prediction directly. In object detection and tracking [9, 67] a lookahead predictor generates the future estimate based on the last predictions fused with the supporting observation. Likewise, in action anticipation a lookahead predictor can be employed to generate a prediction in the action space.

To this end, we propose an inductive attention model, dubbed IAM, which is capable of processing the long video inputs and uses the previous anticipative action prediction as a query to induce possible future actions from experience. We equip IAM with an indexable memory to store past contexts for attention lookup, where each past moment is recorded in a key-value pair formed by representative features and corresponding anticipation scores. Our proposed model natively considers many-to-many associations while computing the correlation between the last prediction and previously predicted action trajectories (stored as the memory keys). As a result, the relevant pre-action durations can be retrieved and associated with anticipating future action. As shown in Figure 1, our model can significantly improve action accuracy over the previous methods. IAM obtains state-of-the-art accuracy on large-scale anticipation datasets, despite using fewer model parameters.

Our proposed IAM recurrently updates the internal states at each video timestep. Empirical findings in previous works [60, 51] showed that addressing the predictive tasks using sequential modeling enables inferring the temporal connection better than with the clip-based approach. A hypothesis behind this is that

recurrent networks can efficiently capture the sequence manifold, which was associated with an inductive bias in previous works [49, 16]. Consequently, transformers designed for action anticipation employ a causal decoder and consume inputs sequentially to encode the sequence dynamics [22, 61]. Furthermore, to address the well-known forgetting problem of recurrent models [27, 12], our model leverages a higher-order recurrent design [50, 51, 56] in the update process, in conjunction with inductive attention and the indexed memory.

2. Related Work

RNNs in Action Anticipation. Recurrent neural networks (RNNs) are commonly used to model the sequence input. Some empirical evidence shows the inductive bias learned by the recurrent models can effectively handle action prediction tasks [60, 51]. Early works on video action anticipation employed LSTM in an encoder-decoder architecture and established the baseline in the video action anticipation problem [18]. Several subsequent improvements are proposed over the baseline, [43] enhanced the original LSTM encoder with an encoder that can handle the spatial-temporal structure; [44] introduced a self-regulated module and achieved accuracy gains by exploiting long-range context features in recurrent updates. In addition, [8] studied using label smoothing to account for future uncertainty and shows improvements. On the other hand, some related works extended the recurrent mechanism, for example, [62, 17] explicitly leveraging future information and simultaneously predicting future frames; [55] leveraged higher-order recurrent and combined with proposed spatial-temporal decomposed attention for action predictions. Moreover, [57] generalized the recurrent mechanism as message-passing learning and analyzed the information propagation in spatial-temporal with self-attention.

Our work also leverages higher-order recurrence in the updates, and incorporates inductive attention to predict future action. As a result, our proposed model can explicitly lookup the previous 30s contexts in each recurrent update to alleviate the forgetting problem in conventional RNNs.

Transformers in Action Anticipation. Transformer architectures have been applied with success in video action recognition [6, 3]. The core element in transformers is self-attention [58], originally introduced for language processing tasks. Later, vision transformers (ViTs) led the trend in various vision tasks [15, 66, 25]. Recent works on action anticipation build upon transformers as a basic model, outperforming recurrent baselines. [22] proposed a transformer model

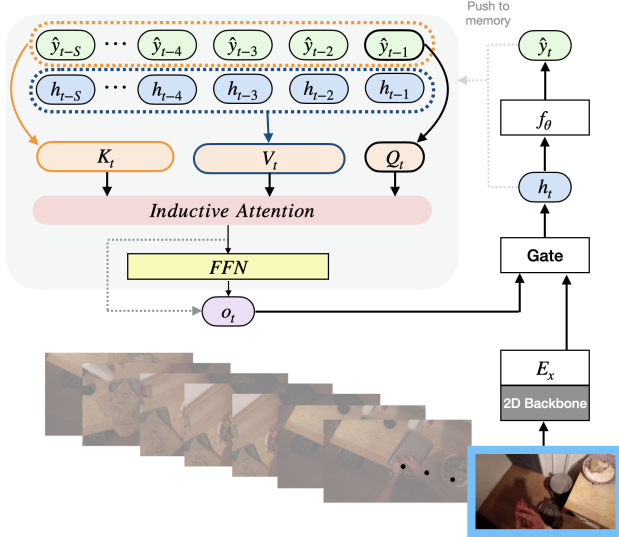


Figure 2. Inductive attention model takes the previous prediction \hat{y}_{t-1} as the query and computes the correlation with memory keys $(\hat{y}_{t-1}, \dots, \hat{y}_{t-S})$ to aggregate a maintained queue of recurrent states $(h_{t-1}, \dots, h_{t-S})$. The output is then fused with the encoded frame input via a gating function and forms the recurrent state h_t to derive the current prediction \hat{y}_t .

solely based on self-attention layers for action anticipation. The model comprises the ViT backbone and the causal decoder to capture the temporal dependencies. [61] proposed a memory compression module for the transformer to model long-range dependencies efficiently and has nearly linear scaling complexity, providing outstanding performance in various video tasks.

Transformer has shown capability in general modeling for sequential inputs [31, 30]. In line with these findings, we deploy attention in our model as a flexible mechanism for distilling temporal context. Our work is also related to the recent progress of combining sequence modeling and attention [28, 29, 7]. These approaches integrate recurrent with self-attention to overcome the quadratic computation complexity of transformers and to learn better representations for recurrent propagation. However, these methods have not yet been extensively evaluated on large datasets nor tested in practical application settings.

3. Preliminaries

Higher-Order Recurrent Networks. Similar to conventional n-gram language model [48], higher-order recurrent networks [50] sequentially compute new outputs and internal states from aggregations of multiple

previous states. It is considered the extension of the (first order) Markov chain assumption behind conventional recurrent networks.

More formally, in a first-order recurrent model, the new internal (hidden) state h_t is computed from the input x_t and a gated version of the previous hidden state, $g(h_{t-1})$, as follows

$$h_t = f(x_t + g(h_{t-1})). \quad (1)$$

In a higher-order recurrent model, multiple past states are referenced and aggregated to predict the new state, by

$$h_t = f(x_t + \phi(h_{t-1}, \dots, h_{t-S})). \quad (2)$$

Here S is a hyper-parameter to specify the number of past states (the order of the model), and function $\phi(\cdot)$ implements the (gated) aggregation in the higher-order model.

There are several choices for the aggregation function ϕ , such as linear function [50], polynomial function [64], convolutional tensor-train decomposition [51], spatial-temporal decomposed attention [55]. In this work, we propose inductive attention to summarizing from the higher-order states.

(Self-)Attention. Attention retrieves the correlation context in the values V by computing the dot-product correlation of keys K conditioned on the query Q . Typically, V and K can be traced back to the same input source, while the query Q is purposely chosen to ensure task-relevant information is retrieved by attention. The standard form of attention [58] is implemented as follows

$$Attention(Q, K, V) = softmax\left(\frac{Q^T K}{\sqrt{d}}\right)V \quad (3)$$

where d denotes the dimension of vectors K and Q . Self-attention refers to the case when Q, K, V are all derived from the same input source. Multi-Head Attention (MHA) further separates the Q, K, V into multiple groups (heads) in parallel and fuses heads with an additional linear transform at the output.

Since the attention layer contains only linear operations, a Feed-Forward Network (FFN) comes in for non-linear layer stacking. FFN is implemented by two fully-connected layers, with the expanding factor of 4 for the bottleneck, and a non-linear activator function *act* placed in between

$$FFN(x) = act(w_1^T norm(x))w_2 + x \quad (4)$$

The widely adopted choice for the normalization (indicated by *norm* in the equation) is layer normalization [4] or RMSNorm [65]. Likewise, GELU [26] for the activator function.

4. Proposed Method

Our Inductive Attention Model (IAM) combines an indexed memory with inductive attention lookup to summarize the video observations in a higher-order recurrent manner. An overview of the proposed architecture is shown in Figure 2.

Indexed Memory. Given the trajectory of previous recurrent state vectors, $h_{t-1}, h_{t-2}, \dots, h_{t-S}$, we introduce an indexed memory to cache the most recent state vectors. The indexed memory is a queue that stores past experiences as key-value pairs. For every timestep t , we project the anticipation prediction $\hat{y}_t \in \mathbb{R}^C$ (C indicates the number of action classes) from a probability distribution to a low dimension vector of size $d/4$ by a function E_K (a dense layer with ReLU), and assign the value by h_t .

$$M_t = \{(E_K(\hat{y}_i), h_i) \text{ for } i = t-1, \dots, t-S\} \quad (5)$$

where S defines the maximal size of the queue (memory capacity). During the training, we stop the gradient of \hat{y}_i in eq (5) to break the dependency from future timesteps.

The indexed memory follows the first-in-first-out (FIFO) update policy. We push the prediction \hat{y}_t and recurrent state h_t at every time t , and pop the oldest element in the queue that exceeds the memory capacity.

Inductive Attention Model. For each timestep $t > 0$, we have a previous prediction \hat{y}_{t-1} and indexed memory $M_t = \{M_t^K, M_t^V\}$, with M_t^K, M_t^V presenting the keys and values stored in the memory.

We prepare Q, K, V for inductive attention as follows. We project \hat{y}_{t-1} from a vector of size C down to a vector of size $d/4$ by a functions E_Q (as on \hat{y}_i with E_K). M_t^K, M_t^V are assigned to K and V , respectively. Inductive Attention, IA , is then defined as follows (for simplicity, we ignore the input embeddings in Multi-Head Attention, MHA):

$$IA(\hat{y}_{t-1}, M_t) := FFN(MHA(Q_t, K_t, V_t)), \quad (6)$$

$$\text{where } Q_t = E_Q(\hat{y}_{t-1}), \quad (7)$$

$$K_t = M_{t-1}^K, \quad (8)$$

$$V_t = M_{t-1}^V, \quad (9)$$

Next, we compute the hidden state h_t from attention and the frame input x_t (x_t is obtained from the video frame using a feature extractor). We also encode x_t to

Algorithm 1 Inductive Attention Model

Given E_x to project input to hidden state of size d ; E_K to compress vector of size C to size $d/4$; $sg(\cdot)$ is stop-gradient.

Initialize $M_0 \leftarrow \emptyset$

for every receiving input x_t **do** $\triangleright t$ for time index.

$e_t \leftarrow E_x(x_t)$

if $t = 0$ **then**

$o_t \leftarrow 0$

else

$o_t \leftarrow IA(\hat{y}_{t-1}, M_t)$ \triangleright eq (6).

end if

$g_t \leftarrow \sigma(w_2^T(\max(0, [o_t; e_t]w_1)))$

$h_t \leftarrow g_t \cdot o_t + (1 - g_t) \cdot e_t$

$\hat{y}_t \leftarrow f_\theta(h_t)$

$M_{t+1} \leftarrow \text{push}(E_K(sg(\hat{y}_t)), h_t)$ to M_t

if M_{t+1} exceeds the maximal capacity **then**

pop the oldest element in M_{t+1}

end if

yield \hat{y}_t

end for

a size d vector by E_x , a dense layer with ReLU.

$$e_t = E_x(x_t) \quad (10)$$

$$o_t = IA(\hat{y}_{t-1}, M_t) \quad (11)$$

$$g_t = \sigma(w_2^T(\max(0, [o_t; e_t]w_1))) \quad (12)$$

$$h_t = g_t \cdot o_t + (1 - g_t) \cdot e_t \quad (13)$$

$$\hat{y}_t = f_\theta(h_t) \quad (14)$$

Here f_θ is an anticipation predictor, parameterized by weights θ , which maps the hidden state into the action distribution. g_t controls the mixture ratio between past experience (the output of inductive attention) and current frame input by feeding the concatenated $[o_t; e_t]$ to an MLP. The MLP uses w_1, w_2 to down-sample and up-sample the input by a factor of 4. The sigmoid function $\sigma(\cdot)$ is to squash values into the range $[0, 1]$. We set $o_t = 0$ for the initial step $t = 0$, when memory is empty. Algorithm 1 summarizes in pseudo-code the forwarding process.

Our model carries out a many-to-many association while computing the dot-product $Q^T K$ in eq (6). By using $Q \equiv \hat{y}_{t-1}$ and $K \equiv [\hat{y}_{t-2}, \dots, \hat{y}_{t-S}]$, it estimates the pairwise correlation between previous predictions of all classes in \hat{y}_* .

Training Objective. Prior works in action anticipation mostly adopted the training scheme from the action recognition setting (Figure 3 left), where a model maps every timestep of an input segment to a global anticipation target. Although training this way might

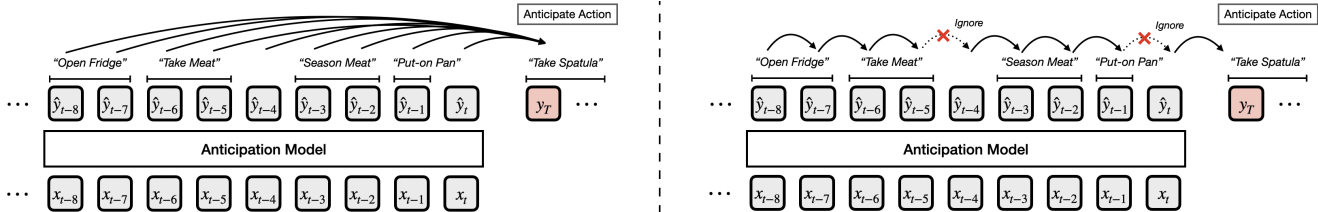


Figure 3. Supervision schemes with example activity. **Conventional learning (left)** uses the target action at the fixed time point as supervision. **Our learning scheme (right)** uses the next action, executed τ_a steps ahead in time, as supervision signal that may change at any step in time. This training scheme mimics the continuous inference scenario.

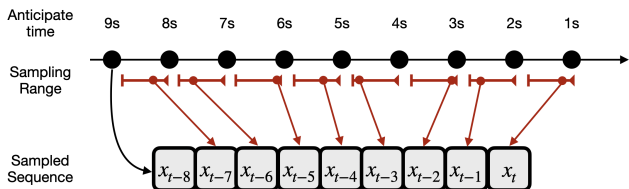


Figure 4. Jitter sampling augmentation replaces each video frame x_t in the train sequence by randomly drawing a source frame from the video segment enclosed by x_{t-1} and x_t . The first frame (i.e., x_{t-8} in the figure) keeps intact to prevent crossing the video boundary.

help capture and map long-range activity trajectories at once to the anticipation target, models could struggle to associate an early action of the input sequence to the future target if they are separated over a long period, e.g., tens of seconds. For instance, consider an activity containing the following actions: "Open Fridge" \rightarrow "Take Meat" \rightarrow "Season Meat" \rightarrow "Put-on Pan" \rightarrow "Take Spatula". The target action "Take Spatula" will have a decreasing connection to its preceding actions that rarely exist between "Open Fridge" and "Take Spatula".

In our training scheme (Figure 3 right), we treat every timestep equally and force the model always to predict the target action that happens in τ_a seconds. τ_a is the anticipation time: it indicates how many seconds after the last observation the action to anticipate will occur, and is defined by the benchmark (e.g., $\tau_a = 1s$ in EPIC-KITCHENS-100). Indeed, the learned knowledge of "Open Fridge" \rightarrow "Take Meat" (subsequent actions at close distance) is assumed to reflect stronger generalization than "Open Fridge" \rightarrow "Take Spatula" (temporally far). We furthermore ignore steps where the interval of length τ_a does not contain any action when computing the training loss. Note that even though in our scheme we supervise the model not at segment level but at the frame level, the temporal

context used to generate the prediction will still enable the model to accumulate enough evidence over time.

Jitter Augmentation. Rather than using the original frame rate in video modeling, a down-sampling is usually performed to lower the frame rate for training efficiency. According to this, we propose jitter augmentation that replaces each video frame x_t in the train sequence by randomly drawing a source frame from the video segment enclosed by x_{t-1} and x_t . For example, given a training video sampled at F_{train} frame-per-seconds (fps) and a source device providing F_{device} fps, we would have $F_{device} - F_{train}$ frames not being utilized at training time. Therefore, we can re-sample the frame index of a training sequence by offsetting $[-(F_{device} - F_{train}), 0]$ for augmentation. Figure 4 demonstrates the jitter augmentation.

5. Experiments

We benchmark our proposed method in three popular egocentric video datasets for action anticipation. The ablation study is presented to validate the design choice in our proposed model.

5.1. Implementation Details

In all experiments, we adopted TSN [19], ConvNeXt [38], and Swin [37] as backbone variants in our model. In all evaluation tables we highlight in gray the methods based on the same feature set for fair comparisons.

We trained our model using AdamW optimizer [39] with a learning rate set to $2e-4$ and a cosine decay scheduler. We set weight decay to $1e-2$ and exclude biases and normalization layers from weight decay. We use batch size 128 and train for 50 epochs on a single NVIDIA RTX 3090 GPU with automatic mixed precision enabled. Throughout this study, our model contains a single IAM layer instantiated with hidden size set to $d = 2048$ for all the internal variables defined in eq (10-13). We used dropout rate 0.6. Other hyperparameters are listed individually for each dataset.

Table 1. EPIC-Kitchens-100 validation result. The performance is measured in mean top-5 report (MT5R) at the $\tau_a = 1s$. Individual actions (A), verbs (V), and nouns (N) accuracy is further presented. Rows which are highlighted in gray color indicate the methods are based on the same backbone features.

Methods	Modality	External Data	Param Counts	Overall Classes			Unseen Classes			Tail Classes		
				A	V	N	A	V	N	A	V	N
TempAgg [47]	RGB, Obj, Flow, ROI	IN1K + EPIC bbox	-	14.7	23.2	31.4	14.5	28.0	26.2	11.8	14.5	22.5
RULSTM [19]	RGB, Obj, Flow	IN1K + EPIC bbox	-	14.0	27.8	30.8	14.2	28.8	27.2	11.1	19.8	22.0
TSN-AVT+ [22]	RGB, Obj	IN21K + EPIC bbox	-	14.8	25.5	31.8	11.5	25.5	23.6	12.6	18.5	25.8
AVT+ [22]	RGB, Obj	IN21K + EPIC bbox	-	15.9	28.2	32.0	11.9	29.5	23.9	14.1	21.1	25.8
chance	-	-	-	0.2	6.4	2.0	0.5	14.4	2.9	0.1	1.6	0.2
TempAgg [47]	RGB	IN1K	-	13.0	24.2	29.8	12.2	27.0	23.0	10.4	16.2	22.9
RULSTM [14]	RGB	IN1K	-	13.3	27.5	29.0	-	-	-	-	-	-
HORST [55]	RGB	IN1K	-	13.2	24.5	30.0	-	-	-	-	-	-
MPNNEL-TB [57]	RGB	IN1K	-	14.8	28.7	31.4	-	-	-	-	-	-
TSN-AVT [22]	RGB	IN1K	-	13.6	27.2	30.7	-	-	-	-	-	-
irCSN152-AVT [22]	RGB	IG65M	-	12.8	25.5	28.1	-	-	-	-	-	-
AVT [22]	RGB	IN1K	378M	13.4	28.2	29.3	-	-	-	-	-	-
AVT [22]	RGB	IN21+1K	378M	14.4	28.7	32.3	-	-	-	-	-	-
AVT [22]	RGB	IN21K	378M	14.9	30.2	31.7	-	-	-	-	-	-
TSN-DCR-LSTM [63]	RGB	IN1K	14M	14.5	27.9	28.0	-	-	-	-	-	-
TSM-DCR-LSTM [63]	RGB	IN1K	20M	15.2	28.4	28.5	-	-	-	-	-	-
TSN-DCR [63]	RGB	IN1K	78M	14.6	31.0	31.1	-	-	-	-	-	-
TSM-DCR [63]	RGB	IN1K	84M	16.1	32.6	32.7	-	-	-	-	-	-
MeMViT 16x4 [61]	RGB	K400	59M	15.1	32.8	33.2	9.8	27.5	21.7	13.2	26.3	27.4
MeMViT 32x3 [61]	RGB	K700	212M	17.7	32.2	37.0	15.2	28.6	27.4	15.5	25.3	31.0
TSN-IAM (Ours)	RGB	IN1K	42M	17.5	32.2	35.7	11.9	31.4	24.9	16.8	26.9	31.8
ConvNeXt-IAM (Ours)	RGB	IN22K	142M	17.6	31.4	36.2	12.0	33.0	25.0	17.1	26.0	32.0
Swin-IAM (Ours)	RGB	IN22K	141M	18.1	32.1	37.2	16.6	34.6	27.9	17.6	26.7	33.0

Table 2. EPIC-Kitchens-55 validation results at the $\tau_a = 1s$. The top-1/top-5 action accuracy and top-5 action recall are summarized. The highlighted rows indicate the fair comparison under the same backbone usage. All methods are done in RGB modality.

Methods	Backbone	External Data	Top-1	Top-5	Recall
RULSTM [18]	TSN	IN1K	13.1	30.8	12.5
TempAgg [47]	TSN	IN1K	12.3	28.5	13.1
ImagineRNN [62]	TSN	IN1K	13.7	31.6	-
SRL [44]	TSN	IN1K	-	31.7	13.2
HORST [55]	TSN	IN1K	12.8	31.6	12.2
MPNNEL-TB [57]	TSN	IN1K	13.8	32.0	13.6
AVT-h [22]	TSN	IN1K	13.1	28.1	13.5
AVT-h [22]	AVT-b	IN21+1K	12.5	30.1	13.6
AVT-h [22]	irCSN152	IG65M	14.4	31.7	13.2
DCR [63]	TSN	IN1K	13.6	30.8	-
DCR [63]	irCSN152	IG65M	15.1	34.0	-
DCR [63]	TSM	IN1K	16.1	33.1	-
IAM (Ours)	TSN	IN1K	13.5	32.1	14.3
IAM (Ours)	ConvNeXt	IN22K	13.3	32.6	15.1
IAM (Ours)	Swin	IN22K	14.2	34.0	16.1

5.2. Datasets

EPIC-Kitchens-100 (EK100) [14]: EK100 is a large-scale egocentric video dataset containing 100 hours of recordings. It includes 3806 action labels consisting of 97 verbs and 300 nouns, which splits into 67217 segments for training and 9668 for validation. Similar to [61] that used an equalized loss for addressing the class imbalance, we rescale the loss weightings proportional to the inverse counts of class occurrences in the training set. We also apply the jitter augmentation described in section 4. Mean top-5

Table 3. EGTEA Gaze+ validation results on the split 1 at the $\tau_a = 0.5s$. We reported the top-1 accuracy and mean top-1 recall of each individual action (A), verb (V) and noun (N). The methods highlighted in background are under the same backbone usage. All methods are based on RGB modality.

Methods	Top-1 Acc			Mean Top-1 Recall		
	A	V	N	A	V	N
I3D-Res50 [10]	34.8	48.0	42.1	23.2	31.3	30.0
FHOI [36]	36.6	49.0	45.5	32.5	32.7	25.3
TSN-AVT-h [22]	39.8	51.7	50.3	28.3	41.2	41.4
AVT [22]	43.0	54.9	52.2	35.2	49.9	48.3
TSN-IAM (Ours)	43.5	54.3	52.2	35.5	43.8	46.6
ConvNeXt-IAM (Ours)	44.6	54.5	53.1	36.3	42.6	45.3
Swin-IAM (Ours)	45.4	55.9	54.3	37.4	46.5	49.3

recall (MT5R) for action, verb, and noun is measured at anticipation interval $\tau_a = 1s$. We sampled each clip of the dataset at 1 fps to obtain 30 frames.

EPIC-Kitchens-55 (EK55) [13]: EK55 contains 55 hours of egocentric video recordings with 2513 action classes comprising 125 verbs and 352 nouns. It includes 23492 segments for training and 4979 for validation. We did not apply the jitter augmentation. Instead, the label smoothing [42] of ratio 0.6 is adopted. Top-1/5 action accuracy and mean top-5 action recall (MT5R) at $\tau_a = 1s$ are reported. We sampled the dataset at 1 fps to obtain 10 frames.

EGTEA Gaze+ [33]: EGTEA Gaze+ is another egocentric video dataset containing more than 28 hours of video recordings. The dataset comes with 10321 seg-

ments annotated with 106 unique action classes. The video segments are further split into 3 folds. We followed the experiment setup in [36, 22], which evaluates on split 1, with 8299 clips for training and 2022 for validation. Anticipation accuracy is assessed at $\tau_a = 0.5s$ for top-1 action accuracy and mean top-1 action recall. We adopted label smoothing with a ratio of 0.4 and sampled the dataset at 2 fps to obtain 10 frames.

5.3. EK100 Action Anticipation Result

We compared our proposed model (IAM) with prior works on the EK100 dataset and summarized the results in Table 1. In addition, methods using pre-extracted TSN features from the dataset developers are highlighted (in gray background color) for fair comparisons. Our proposed model outperforms those methods by a large margin. We obtained +2.7 gains in mean top-5 recall in overall action accuracy, -0.3 in unseen action classes, and +6.4 in tail action classes. Although slightly lower unseen action accuracy has been observed, much better verb (+4.4) and noun (+1.9) predictions were achieved. In brief, using pre-extracted TSN features significantly improves over some strong baselines, including the previous top-rank competition winner AVT, and is competitive with the state-of-the-art MeMViT.

Furthermore, by replacing the TSN with recent ConvNeXt (convolutional-based) and Swin (transformer-based) backbones, IAM outperforms MeMViT by a significant margin: +0.4 in overall classes, +1.4 in unseen classes, and +2.1 in tail classes. Moreover, our method is with fewer model parameters. Figure 1 shows the efficiency and efficacy of the proposed IAM on the EK100 evaluation.

5.4. EK55 Action Anticipation Result

Table 2 summarizes the performance comparisons of our model and prior works on the EK55 benchmark. TempAgg [47] leveraged multi-scale temporal information and aggregate for the action anticipation; SRL [44] enhanced the recurrent update by re-attend the past observations; HORST [55], MPNNEL-TB [57] consider the spatial-temporal information in recurrent modeling; ImagineRNN [62] generate the future frame to guide the prediction; DCR [63] introduces a curriculum learning scheme and additional pretraining improvements.

The evaluation results show our model outperforms others on the top-5 action accuracy and mean top-5 recall based on the same TSN baseline. We achieve further performance gains while using ConvNeXt and Swin as feature extractors. Like the EK100 evaluation, our model with the Swin backbone achieved the best

Table 4. Ablation on using different input lengths. The experiment is done on EPIC-Kitchens-100 dataset and measured in mean top-5 recall (MT5R).

Input Length	10s	20s	30s	40s	50s	60s
MT5R (%)	16.9	17.5	17.5	17.3	16.7	16.7

Table 5. Ablation on jitter sampling augmentation. The accuracy and recall defined in each dataset are different, in which action top-5 is used for EK55/100, and top-1 for EGTEA Gaze+.

Dataset	Input	Jitter Sampling	Action Accuracy	Action Recall
EK100	30 frames @ 1fps	✓	24.7 27.3	16.9
EK55	10 frames @ 1fps	✓	31.6 32.1	13.9 14.3
EGTEA Gaze+	10 frames @ 2fps	✓	43.2 43.5	36.0 35.5

overall performance. Note that AVT-h on the ViT-based AVT-b backbone does not perform better in accuracy, unlike in EK100, than AVT-h with the convolutional backbone irCSN152 pre-trained on IG65M, indicating the AVT does not produce consistent scores by one specific backbone across different datasets. On the other hand, DCR achieved higher top-1 accuracy, a possible gain via their curriculum learning from the future frames. This observation exposes the emergence of an appropriate pretraining method for video predictive tasks. We mark it as a future direction.

5.5. EGTEA Gaze+ Action Anticipation Result

We also evaluated our model on the EGTEA Gaze+ egocentric video dataset. Table 3 includes the task baselines, where I3D-Res50 [10] proposed a clip-based 3D convolutions model; FHOI [36] utilizes the hand movements using a 2D resnet-50 backbone; and the previous state-of-the-art AVT. The results show that models based on sequential or recurrent networks outperform clip-based models, confirming the conclusions drawn in [60, 51].

Based on the same pre-extracted TSN features, our model significantly improves top-1 action accuracy and top-1 action recall over the TSN-AVT. Furthermore, we achieve state-of-the-art action accuracy when using the recent ConvNeXt or Swin transformer as backbone.

5.6. Ablation Study

This section analyzes the optimal input length for IAM. In addition, the effect of jitter augmentation and the selection of the query are also covered. All the experiments are done on EK100 using the pre-extracted baseline TSN features.

Input Length. We first evaluated the performance using different lengths of inputs, ranging from 10 to 60 seconds. The longer input length implies more pre-action trajectories in each training sequence. Table 4 shows that our model reaches peak performance when fed with 20 to 30 seconds inputs and shows degradation when either increasing or decreasing the length. This result reveals that the model does not always have increasing performance while extending the contexts. A similar conclusion can also be found in the preliminary study [18]. However, the optimal input length for our model is significantly longer than earlier recurrent models have been reported. This evidence demonstrates that our higher-order inductive attention can effectively utilize historical experience in long video observations. In addition, compared with the previous higher-order recurrent networks, we significantly extended from 3-8 higher-order states to the 30 without suffering from gradient instability during learning. On the other hand, [61] suggested taking long video inputs (longer than a minute) can improve the recognition performance of models. Our model based on recurrent mechanisms can reach equal or even better accuracy in the length of the same or shorter input with higher efficiency. This finding demonstrates the difference between sequential and recurrent modeling.

We analyze the memory footprint of our proposed indexed memory, which caches up to S elements of hidden dimension size d . Each element needs $d/4$ for key and d for value, totalling $(5/4)dS$. Consider our model with $S = 30$ and $d = 2048$. Under a single precision floating point, it only occupies about 300 KB during runtime inference, showing the resource impact of memory capacity is negligible in practice.

Jitter Augmentation. We validate the jitter augmentation described in section 4 on different datasets in Table 5. Overall, the proposed jitter augmentation increased the overall action recall (for 2 out of the 3 entries) but at the cost of accuracy (for 3 out of 3). The jitter augmentation varied the sampling rate during training, which is equivalent to randomly increasing τ_a to $\widehat{\tau}_a \in [\tau_a, 2\tau_a)$. This makes the task more challenging, and the accuracy of the action is adversely affected. On the other hand, it encourages the model to consider more diverse responses. According to the trade-off between precision and recall, we suggest optionally applying jitter augmentation for the needs of different scenarios.

About Query. Finally, we show that using task prediction as the query in inductive attention can improve overall performance.

Table 6. EK100 performance comparison using different choices for the query. The numbers are measured in mean top-5 recall (MT5R) for actions (A), verbs (V), nouns (N).

Query	Overall Classes			Unseen Classes			Tail Classes		
	A	V	N	A	V	N	A	V	N
Frame Input	17.0	31.1	35.7	11.1	27.4	24.9	16.4	25.6	32.1
Last Pred.	17.5	32.2	35.7	11.9	31.4	24.9	16.8	26.9	31.8
Δ	+0.5	+1.1	+0.0	+0.8	+4.0	+0.0	+0.4	+1.3	-0.3

Table 7. EK55 performance comparison using different query choices, in which frame features or previous predictions in our model.

Query	Top-1	Top-5	Recall
Frame Input	13.2	31.4	13.9
Last Pred.	13.5	32.1	14.3
Δ	+0.3	+0.7	+0.4

Table 8. EGTEA Gaze+ performance comparison using different query choices, in which frame features or previous predictions in our model.

Query	Top-1 Acc			Mean Top-1 Recall		
	A	V	N	A	V	N
Frame Input	43.0	54.2	51.7	34.5	44.9	45.8
Last Pred.	43.5	54.3	52.2	35.5	43.8	46.6
Δ	+0.5	+0.1	+0.5	+1.0	-1.1	+0.8

Table 6 compares the results on the EK100 dataset. In the experiment with frame features as the query, we replace the prediction \hat{y}_{t-1} in eq. (6) with frame input x_t and remove the encoding modules (E_Q, E_K in eq. (7)(5)). Using the last prediction as the query can achieve overall consistent improvement. A slight degradation on the tail class nouns is found, which may be attributed to the fact that frame input features contain more spatial information than task predictions. Overall, inductive attention with the last prediction as query improves over the verb classes by a margin.

Similarly, the general improvements using the last prediction query are shown in Tables 7 and 8. By combining our higher order recurrent model design with self-attention and utilizing previous prediction as the query, IAM obtains state-of-the-art performance in three action anticipation benchmarks.

6. Conclusion

This paper introduced IAM, an Inductive Attention Model for video action anticipation. IAM leverages a higher-order recurrent design to summarize the temporal information efficiently, and induces from historical moments stored in the indexed memory to infer the future action. Utilizing previous predictions as the query in inductive attention allows the proposed model to handle long videos and set new state-of-the-art accuracy on large-scale egocentric video datasets. Our method delivers higher accuracy and efficiency while requiring fewer model parameters than previous works.

References

- [1] Mohammad Sadegh Ali Akbarian, Fatemehsadat Saleh, Mathieu Salzmann, Basura Fernando, Lars Petersson, and Lars Andersson. Encouraging lstms to anticipate actions very early. In *ICCV*, pages 280–289, 2017. **1**
- [2] Ben Anderson. Preemption, precaution, preparedness: Anticipatory action and future geographies. *Progress in human geography*, 34(6):777–798, 2010. **1**
- [3] Anurag Arnab, Mostafa Dehghani, Georg Heigold, Chen Sun, Mario Lučić, and Cordelia Schmid. Vivit: A video vision transformer. In *Proceedings of the IEEE/CVF International Conference on Computer Vision*, pages 6836–6846, 2021. **2**
- [4] Jimmy Lei Ba, Jamie Ryan Kiros, and Geoffrey E Hinton. Layer normalization. *arXiv preprint arXiv:1607.06450*, 2016. **3**
- [5] Gedas Bertasius, Heng Wang, and Lorenzo Torresani. Is space-time attention all you need for video understanding? In Marina Meila and Tong Zhang, editors, *Proceedings of the 38th International Conference on Machine Learning, ICML 2021, 18-24 July 2021, Virtual Event*, volume 139 of *Proceedings of Machine Learning Research*, pages 813–824. PMLR, 2021. **1**
- [6] Gedas Bertasius, Heng Wang, and Lorenzo Torresani. Is space-time attention all you need for video understanding? In *ICML*, volume 2, page 4, 2021. **2**
- [7] Aydar Bulatov, Yuri Kuratov, and Mikhail S. Burtsev. Recurrent memory transformer. *CoRR*, abs/2207.06881, 2022. **3**
- [8] Guglielmo Camporese, Pasquale Coscia, Antonino Furnari, Giovanni Maria Farinella, and Lamberto Ballan. Knowledge distillation for action anticipation via label smoothing. In *2020 25th International Conference on Pattern Recognition (ICPR)*, pages 3312–3319. IEEE, 2021. **2**
- [9] Nicolas Carion, Francisco Massa, Gabriel Synnaeve, Nicolas Usunier, Alexander Kirillov, and Sergey Zagoruyko. End-to-end object detection with transformers. In *Computer Vision—ECCV 2020: 16th European Conference, Glasgow, UK, August 23–28, 2020, Proceedings, Part I 16*, pages 213–229. Springer, 2020. **2**
- [10] Joao Carreira and Andrew Zisserman. Quo vadis, action recognition? a new model and the kinetics dataset. In *proceedings of the IEEE Conference on Computer Vision and Pattern Recognition*, pages 6299–6308, 2017. **6, 7**
- [11] Yunpeng Chen, Yannis Kalantidis, Jianshu Li, Shuicheng Yan, and Jiashi Feng. A²-nets: Double attention networks. In *NeurIPS*, pages 350–359, 2018. **1**
- [12] Junyoung Chung, Caglar Gulcehre, KyungHyun Cho, and Yoshua Bengio. Empirical evaluation of gated recurrent neural networks on sequence modeling. *arXiv preprint arXiv:1412.3555*, 2014. **2**
- [13] Dima Damen, Hazel Doughty, Giovanni Maria Farinella, Sanja Fidler, Antonino Furnari, Evangelos Kazakos, Davide Moltisanti, Jonathan Munro, Toby Perrett, Will Price, et al. Scaling egocentric vision: The epic-kitchens dataset. In *Proceedings of the European Conference on Computer Vision (ECCV)*, pages 720–736, 2018. **6**
- [14] Dima Damen, Hazel Doughty, Giovanni Maria Farinella, Antonino Furnari, Evangelos Kazakos, Jian Ma, Davide Moltisanti, Jonathan Munro, Toby Perrett, Will Price, et al. Rescaling egocentric vision: collection, pipeline and challenges for epic-kitchens-100. *International Journal of Computer Vision*, 130(1):33–55, 2022. **6**
- [15] Alexey Dosovitskiy, Lucas Beyer, Alexander Kolesnikov, Dirk Weissenborn, Xiaohua Zhai, Thomas Unterthiner, Mostafa Dehghani, Matthias Minderer, Georg Heigold, Sylvain Gelly, et al. An image is worth 16x16 words: Transformers for image recognition at scale. *arXiv preprint arXiv:2010.11929*, 2020. **2**
- [16] Reuben Feinman and Brenden M Lake. Learning inductive biases with simple neural networks. In *40th Annual Meeting of the Cognitive Science Society: Changing Minds, CogSci 2018*, pages 1657–1662. The Cognitive Science Society, 2018. **2**
- [17] Basura Fernando and Samitha Herath. Anticipating human actions by correlating past with the future with jaccard similarity measures. In *Proceedings of the IEEE/CVF Conference on Computer Vision and Pattern Recognition*, pages 13224–13233, 2021. **2**
- [18] Antonino Furnari and Giovanni Maria Farinella. Rolling-unrolling lstms for action anticipation from first-person video. *IEEE transactions on pattern analysis and machine intelligence*, 43(11):4021–4036, 2020. **2, 6, 8**
- [19] Antonino Furnari and Giovanni Maria Farinella. Rolling-unrolling lstms for action anticipation from first-person video. *IEEE Transactions on Pattern Analysis and Machine Intelligence (PAMI)*, 2020. **5, 6**
- [20] Roeland De Geest and Tinne Tuytelaars. Modeling temporal structure with LSTM for online action detection. pages 1549–1557, 2018. **1**
- [21] Rohit Girdhar, João Carreira, Carl Doersch, and Andrew Zisserman. Video action transformer network. In *CVPR*, pages 244–253, 2019. **1**
- [22] Rohit Girdhar and Kristen Grauman. Anticipative video transformer. In *Proceedings of the IEEE/CVF International Conference on Computer Vision*, pages 13505–13515, 2021. **2, 6, 7**
- [23] Rohit Girdhar and Deva Ramanan. Attentional pooling for action recognition. In *NeurIPS*, pages 34–45, 2017. **1**
- [24] Peter M Gollwitzer. Action phases and mind-sets. *Handbook of motivation and cognition: Foundations of social behavior*, 2:53–92, 1990. **1**
- [25] Kai Han, Yunhe Wang, Hanting Chen, Xinghao Chen, Jianyuan Guo, Zhenhua Liu, Yehui Tang, An Xiao,

- Chunjing Xu, Yixing Xu, et al. A survey on vision transformer. *IEEE transactions on pattern analysis and machine intelligence*, 2022. **2**
- [26] Dan Hendrycks and Kevin Gimpel. Gaussian error linear units (gelus). *arXiv preprint arXiv:1606.08415*, 2016. **3**
- [27] Sepp Hochreiter and Jürgen Schmidhuber. Long short-term memory. *Neural computation*, 9(8):1735–1780, 1997. **2**
- [28] Feiqing Huang, Kexin Lu, CAI Yuxi, Zhen Qin, Yanwen Fang, Guangjian Tian, and Guodong Li. Encoding recurrence into transformers. In *The Eleventh International Conference on Learning Representations*. **3**
- [29] DeLesley Hutchins, Imanol Schlag, Yuhuai Wu, Ethan Dyer, and Behnam Neyshabur. Block-recurrent transformers. *CoRR*, abs/2203.07852, 2022. **3**
- [30] Andrew Jaegle, Sebastian Borgeaud, Jean-Baptiste Alayrac, Carl Doersch, Catalin Ionescu, David Ding, Skanda Koppula, Daniel Zoran, Andrew Brock, Evan Shelhamer, et al. Perceiver io: A general architecture for structured inputs & outputs. *arXiv preprint arXiv:2107.14795*, 2021. **3**
- [31] Andrew Jaegle, Felix Gimeno, Andy Brock, Oriol Vinyals, Andrew Zisserman, and Joao Carreira. Perceiver: General perception with iterative attention. In *International conference on machine learning*, pages 4651–4664. PMLR, 2021. **3**
- [32] Yu Kong, Zhiqiang Tao, and Yun Fu. Deep sequential context networks for action prediction. In *CVPR*, pages 3662–3670, 2017. **1**
- [33] Yin Li, Miao Liu, and James M Rehg. In the eye of beholder: Joint learning of gaze and actions in first person video. In *Proceedings of the European conference on computer vision (ECCV)*, pages 619–635, 2018. **6**
- [34] Zhenyang Li, Kirill Gavriluk, Efstratios Gavves, Mihir Jain, and Cees G. M. Snoek. Videolstm convolves, attends and flows for action recognition. 166:41–50, 2018. **1**
- [35] Ji Lin, Chuang Gan, and Song Han. TSM: temporal shift module for efficient video understanding. In *ICCV*, pages 7082–7092, 2019. **1**
- [36] Miao Liu, Siyu Tang, Yin Li, and James M Rehg. Forecasting human-object interaction: joint prediction of motor attention and actions in first person video. In *European Conference on Computer Vision*, pages 704–721. Springer, 2020. **6, 7**
- [37] Ze Liu, Yutong Lin, Yue Cao, Han Hu, Yixuan Wei, Zheng Zhang, Stephen Lin, and Baining Guo. Swin transformer: Hierarchical vision transformer using shifted windows. In *Proceedings of the IEEE/CVF international conference on computer vision*, pages 10012–10022, 2021. **5**
- [38] Zhuang Liu, Hanzi Mao, Chao-Yuan Wu, Christoph Feichtenhofer, Trevor Darrell, and Saining Xie. A convnet for the 2020s. In *Proceedings of the IEEE/CVF Conference on Computer Vision and Pattern Recognition*, pages 11976–11986, 2022. **5**
- [39] Ilya Loshchilov and Frank Hutter. Decoupled weight decay regularization. *arXiv preprint arXiv:1711.05101*, 2017. **5**
- [40] Shugao Ma, Leonid Sigal, and Stan Sclaroff. Learning activity progression in lstms for activity detection and early detection. In *CVPR*, pages 1942–1950, 2016. **1**
- [41] Davide Moltisanti, Michael Wray, Walterio Mayol-Cuevas, and Dima Damen. Trespassing the boundaries: Labeling temporal bounds for object interactions in egocentric video. In *Proceedings of the IEEE International Conference on Computer Vision*, pages 2886–2894, 2017. **1**
- [42] Rafael Müller, Simon Kornblith, and Geoffrey E Hinton. When does label smoothing help? *Advances in neural information processing systems*, 32, 2019. **6**
- [43] Nada Osman, Guglielmo Camporese, Pasquale Coscia, and Lamberto Ballan. Slowfast rolling-unrolling lstms for action anticipation in egocentric videos. In *Proceedings of the IEEE/CVF International Conference on Computer Vision*, pages 3437–3445, 2021. **2**
- [44] Zhaobo Qi, Shuhui Wang, Chi Su, Li Su, Qingming Huang, and Qi Tian. Self-regulated learning for egocentric video activity anticipation. *IEEE Transactions on Pattern Analysis and Machine Intelligence*, 2021. **2, 6, 7**
- [45] Louise Reid. Anticipating technology-enabled care at home. *Transactions of the Institute of British Geographers*, 47(1):108–122, 2022. **1**
- [46] Paolo F Ricci, Dave Rice, John Ziagos, and Louis A Cox Jr. Precaution, uncertainty and causation in environmental decisions. *Environment International*, 29(1):1–19, 2003. **1**
- [47] Fadime Sener, Dipika Singhania, and Angela Yao. Temporal aggregate representations for long-range video understanding. In *European Conference on Computer Vision*, pages 154–171. Springer, 2020. **6, 7**
- [48] Claude Elwood Shannon. A mathematical theory of communication. *The Bell system technical journal*, 27(3):379–423, 1948. **3**
- [49] Sean Snyders and Christian W Omlin. Inductive bias in recurrent neural networks. In *Connectionist Models of Neurons, Learning Processes, and Artificial Intelligence: 6th International Work-Conference on Artificial and Natural Neural Networks, IWANN 2001 Granada, Spain, June 13–15, 2001 Proceedings, Part 1 6*, pages 339–346. Springer, 2001. **2**
- [50] Rohollah Soltani and Hui Jiang. Higher order recurrent neural networks. *arXiv preprint arXiv:1605.00064*, 2016. **2, 3**
- [51] Jiahao Su, Wonmin Byeon, Jean Kossaifi, Furong Huang, Jan Kautz, and Anima Anandkumar. Convolutional tensor-train lstm for spatio-temporal learning. *Advances in Neural Information Processing Systems*, 33:13714–13726, 2020. **1, 2, 3, 7**
- [52] Swathikiran Sudhakaran, Sergio Escalera, and Oswald Lanz. LSTA: long short-term attention for egocentric action recognition. In *CVPR*, pages 9954–9963, 2019. **1**

- [53] Swathikiran Sudhakaran, Sergio Escalera, and Oswald Lanz. Gate-shift networks for video action recognition. In *CVPR*, pages 1099–1108, 2020. 1
- [54] Swathikiran Sudhakaran, Sergio Escalera, and Oswald Lanz. Learning to recognize actions on objects in ego-centric video with attention dictionaries. *IEEE Transactions on Pattern Analysis and Machine Intelligence*, 2021. 1
- [55] Tsung-Ming Tai, Giuseppe Fiameni, Cheng-Kuang Lee, and Oswald Lanz. Higher order recurrent space-time transformer for video action prediction. *arXiv preprint arXiv:2104.08665*, 2021. 2, 3, 6, 7
- [56] Tsung-Ming Tai, Giuseppe Fiameni, Cheng-Kuang Lee, and Oswald Lanz. Higher-order recurrent network with space-time attention for video early action recognition. In *2022 IEEE International Conference on Image Processing (ICIP)*, pages 1631–1635. IEEE, 2022. 2
- [57] Tsung-Ming Tai, Giuseppe Fiameni, Cheng-Kuang Lee, Simon See, and Oswald Lanz. Unified recurrence modeling for video action anticipation. *arXiv preprint arXiv:2206.01009*, 2022. 2, 6, 7
- [58] Ashish Vaswani, Noam Shazeer, Niki Parmar, Jakob Uszkoreit, Llion Jones, Aidan N Gomez, Łukasz Kaiser, and Illia Polosukhin. Attention is all you need. *Advances in neural information processing systems*, 30, 2017. 2, 3
- [59] Xiaolong Wang, Ross B. Girshick, Abhinav Gupta, and Kaiming He. Non-local neural networks. In *CVPR*, pages 7794–7803, 2018. 1
- [60] Yunbo Wang, Lu Jiang, Ming-Hsuan Yang, Li-Jia Li, Mingsheng Long, and Li Fei-Fei. Eidetic 3d lstm: A model for video prediction and beyond. In *International conference on learning representations*, 2018. 1, 2, 7
- [61] Chao-Yuan Wu, Yanghao Li, Karttikeya Mangalam, Haoqi Fan, Bo Xiong, Jitendra Malik, and Christoph Feichtenhofer. Memvit: Memory-augmented multi-scale vision transformer for efficient long-term video recognition. In *Proceedings of the IEEE/CVF Conference on Computer Vision and Pattern Recognition*, pages 13587–13597, 2022. 2, 3, 6, 8
- [62] Yu Wu, Linchao Zhu, Xiaohan Wang, Yi Yang, and Fei Wu. Learning to anticipate egocentric actions by imagination. *IEEE Transactions on Image Processing*, 30:1143–1152, 2020. 2, 6, 7
- [63] Xinyu Xu, Yong-Lu Li, and Cewu Lu. Learning to anticipate future with dynamic context removal. In *Proceedings of the IEEE/CVF Conference on Computer Vision and Pattern Recognition*, pages 12734–12744, 2022. 6, 7
- [64] Rose Yu, Stephan Zheng, Anima Anandkumar, and Yisong Yue. Long-term forecasting using tensor-train rnns. *Arxiv*, 2017. 3
- [65] Biao Zhang and Rico Sennrich. Root mean square layer normalization. *Advances in Neural Information Processing Systems*, 32, 2019. 3
- [66] Daquan Zhou, Bingyi Kang, Xiaojie Jin, Linjie Yang, Xiao Chen Lian, Zihang Jiang, Qibin Hou, and Jiashi Feng. Deepvit: Towards deeper vision transformer. *arXiv preprint arXiv:2103.11886*, 2021. 2
- [67] Xizhou Zhu, Weijie Su, Lewei Lu, Bin Li, Xiaogang Wang, and Jifeng Dai. Deformable detr: Deformable transformers for end-to-end object detection. In *International Conference on Learning Representations*, 2020. 2

A. Input Preprocessing

For the TSN baseline used in three action anticipation benchmarks of Table 1,2,3 in the main paper, we downloaded the pre-extracted features from the official release of the EPIC-Kitchens websites¹. TSN is based on the BN-Inception backbone and extracts RGB frame input in size (456, 256). Swin and Convnext implementation and pretrained weights used to present the results in Table 1,2,3 are inherited from the open-source implementation². The frame inputs for Swin and ConvNeXt are (224, 224) in size, with values rescaled to the range [-1, 1].

B. Qualitative Analysis

We draw success and failure cases of our model from EPIC-Kitchens-55/100 and EGTEA Gaze+ datasets for qualitative analysis. We illustrated four video clips, labeled (a) to (d), for the case that the ground truth falls in the model top-5 predictions at the last frame. Also, another four examples, labeled (e) to (h), failed to anticipate the target action. We presented the last eight frames for each video sample and the corresponding top-5 predictions per frame. The figures are best viewed horizontally and zoom-in.

EPIC-Kitchens-100. Figure 5 and 6 show the samples drawn from the EPIC-Kitchens-100 dataset. We can observe that the model can narrow to the specific verbs of activities based on the context. For example, in video (a), predictions converge to verb "wash" or "squeeze". In addition, video (b) recognized "milk" in the first four frames and then switched to the (possible) consequence object "cereal". The video (c) contains minimal movements in the scene change of cooking activity; as a result, our model consistently adhered to relevant predictions but struggled to anticipate the object until the last moment. Moreover, video (d) shows a challenging example where the subject's intention is vague during the entire observation timespan.

Figure 6 reveals some cases our model failed to anticipate. For example, in the video (e), although the model grabs the correct verb, a wrong noun "pizza" is consistently predicted. Other examples can be interpreted as wrong predictions due to a lack of visual observations (e.g., (f)), and due to too many possibilities to narrow the objects (e.g., (g), (h)).

EPIC-Kitchens-55. Figure 7 shows successful cases with the last eight frames that the model observed.

Note that the target noun object in videos (a) and (b) are invisible. However, the model can infer correctly based on past predictions propagated by inductive attention. Furthermore, video (c) requires the model to catch the object "plate" that appears in the first three frames (it goes out of view in the rest of the frames); our model successfully captures the hint. Finally, video (d) holds the prediction results relevant to cooking pasta.

On the other hand, the sample (e) contains no hint about the anticipated object "tofu" and predicts "container" instead. Similarly, there are some mispredicted nouns found in videos (f) and (h); and verbs in (g).

EGTEA Gaze+. We highlight the video (b) in Figure 9, where the prediction can only be issued correctly by being aware of *tomato:container* which only appears in the first two frames, that is six frames away from the last frame. Also, video (c) is with the subtle movement about the *bread:container*. Note how it was taken out and then put back in the last three frames.

Figure 10 reveals some incorrect predictions, primarily due to the insufficient evidence that can be found in the observations (e.g., (e) and (f)), or due to too many possibilities (e.g., (g)); however, note the confidence on verbs), or mixtures in (h).

¹<https://github.com/epic-kitchens/C3-Action-Anticipation>

²<https://github.com/huggingface/pytorch-image-models>, v0.5.4

Time



Figure 5. Some **correct** predictions illustrates on the **EPIC-Kitchens-100** validation set. The figure shows four video clips (the last eight frames presented) and the corresponding top-5 action anticipations ($\tau_a = 1s$). The ground truth is highlighted in bold green.

Time ↑

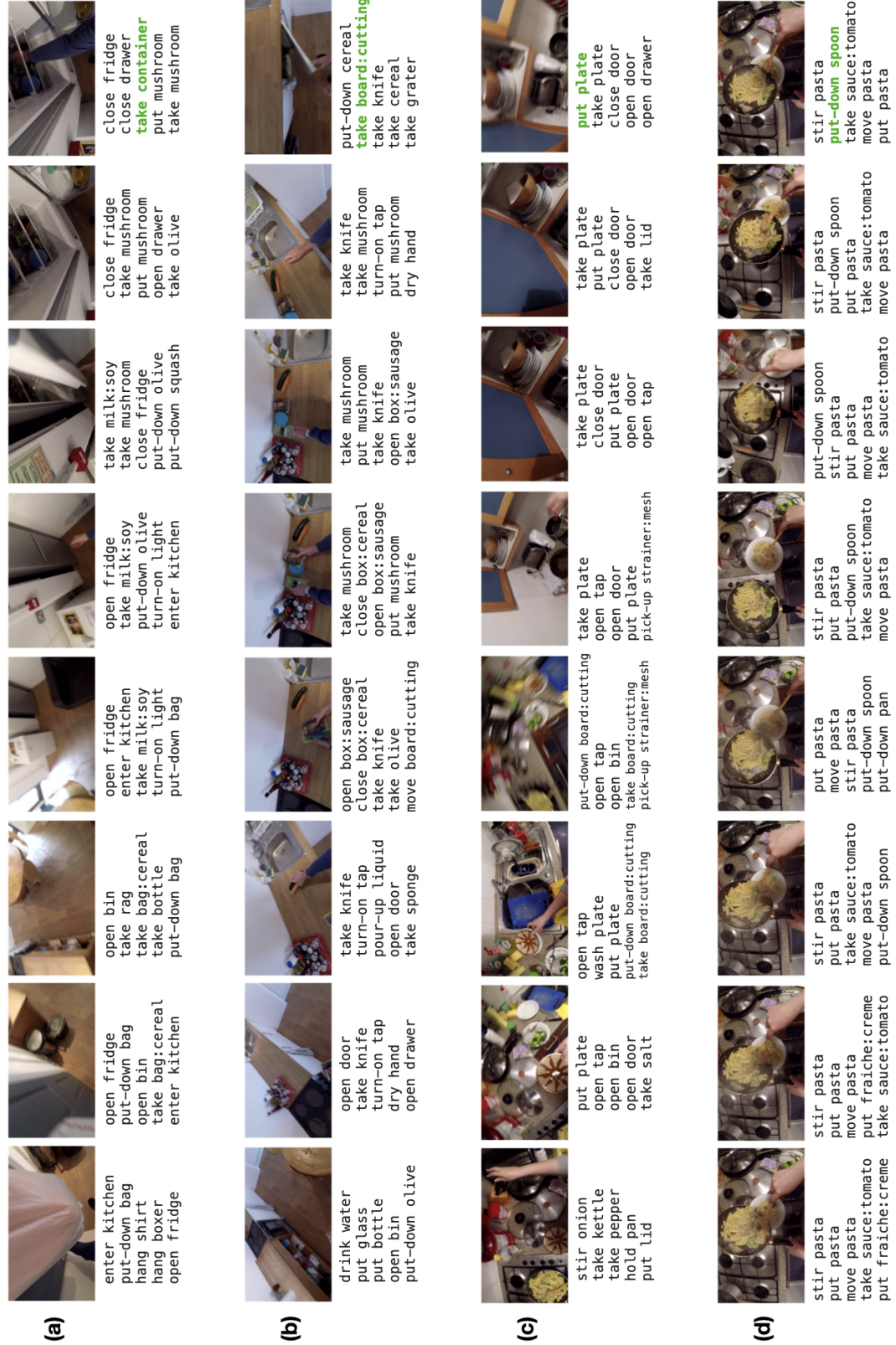


Figure 7. Some **correct** predictions illustrates on the **EPIC-Kitchens-55** validation set. The figure shows four video clips (the last eight frames presented) and the corresponding top-5 action anticipations ($\tau_a = 1s$). The ground truth is highlighted in bold green.



Figure 8. Some **incorrect** predictions illustrates on the **EPIC-Kitchens-55** validation set. The figure shows four video clips (the last eight frames presented) and the corresponding top-5 action anticipations ($\tau_a = 1s$). The ground truth is revealed at the end. The correct verb and noun of action are highlighted in green.

Time ↑

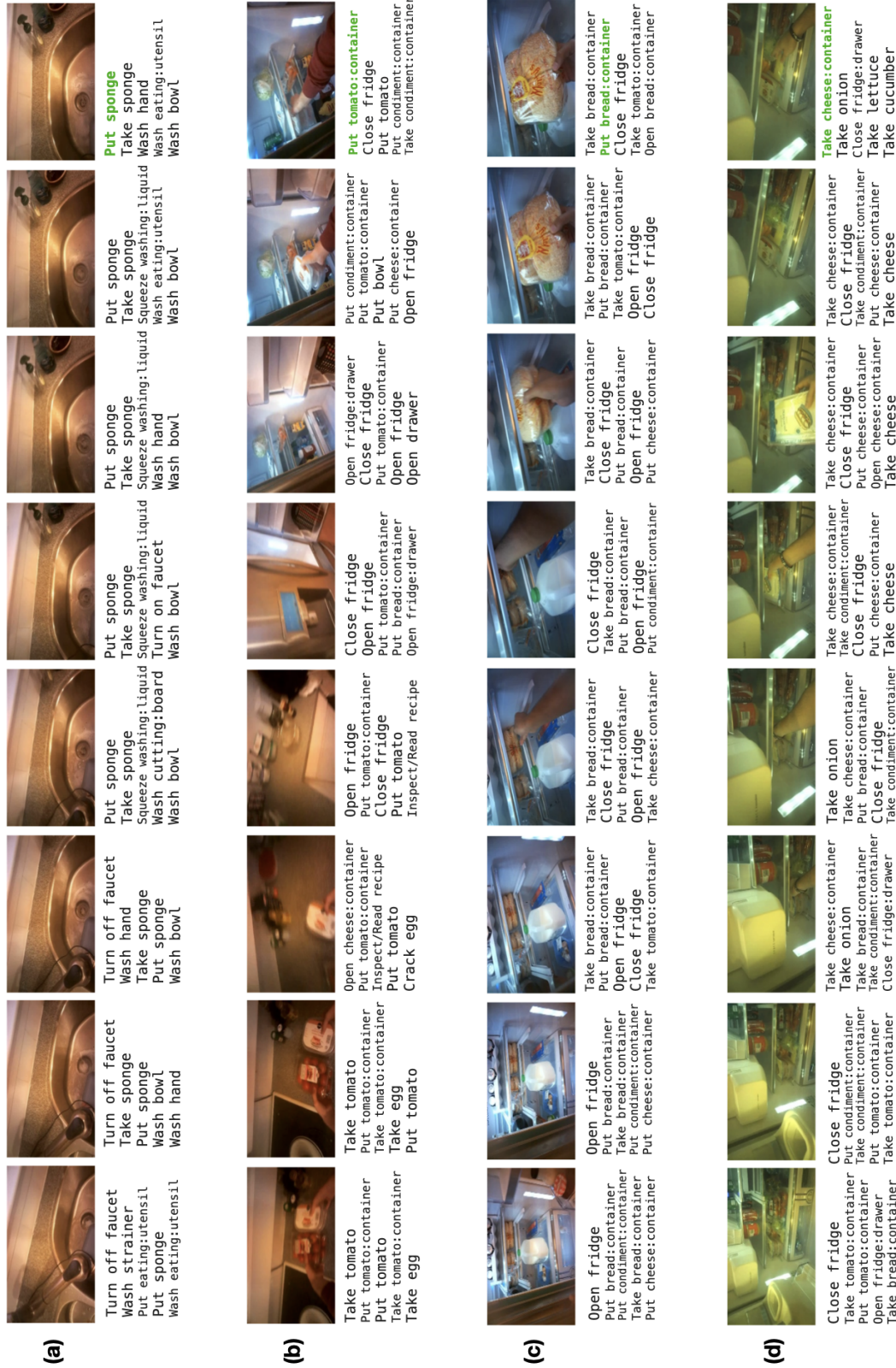


Figure 9. Some **correct** predictions illustrates on the **EGTEA Gaze+** validation set. The figure shows four video clips (the last eight frames presented) and the corresponding top-5 action anticipations ($\tau_a = 0.5s$). The ground truth is highlighted in bold green.

Time ↑

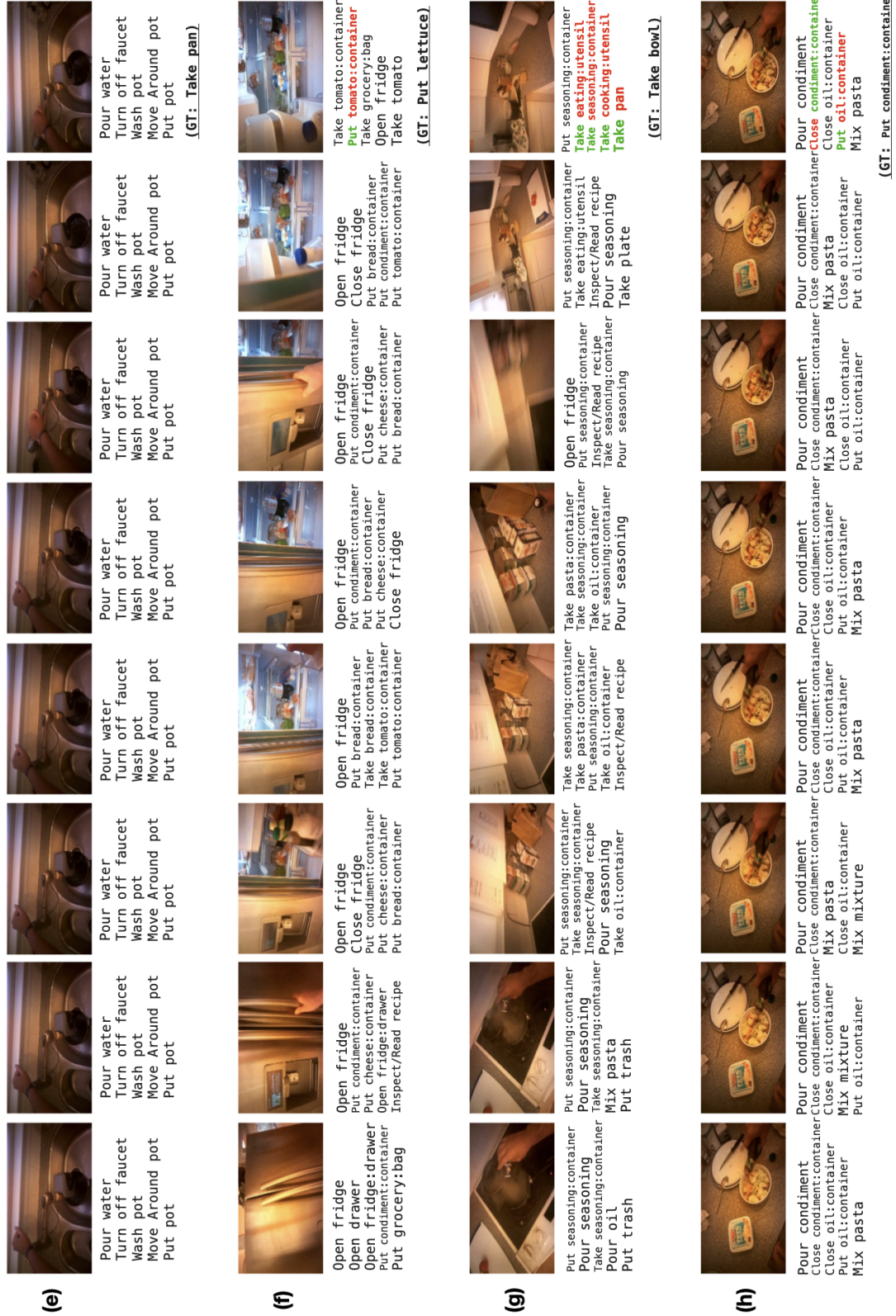


Figure 10. Some incorrect predictions illustrates on the EGTEA Gaze+ validation set. The figure shows four video clips (the last eight frames presented) and the corresponding top-5 action anticipations ($\tau_a = 0.5s$). The ground truth is revealed at the end. The correct verb and noun of action are highlighted in green.